Journal of Sound and Vibration (2001) **246**(2), 297–317
doi:10.1006/jsvi.2001.3632, available online at http://www.idealibrary.com on IDEAL®

NATURAL FREQUENCY CHANGES OF A CRACKED TIMOSHENKO BEAM BY MODIFIED FOURIER SERIES

D. Y. Zheng and S. C. Fan

School of Civil and Structural Engineering, Nanyang Technological University, Nanyang Avenue, Singapore 639798, *Singapore. E-mail: cdyzheng@ntu.edu.sg, cfansc@ntu.edu.sg*

(*Received* 1 *June* 2000, *and in final form* 29 *January* 2001)

A new method is presented in this paper for computing the natural frequencies of a Timoshenko beam with an arbitrary number of transverse open cracks. The essence of this new method lies in the use of a kind of modified Fourier series (MFS) which is developed particularly for a Timoshenko beam having an arbitrary number of transverse open cracks. Unlike the conventional Fourier series, the modified Fourier series can approach a function with internal geometrical discontinuities. Based on the modified Fourier series, one can treat the cracked Timoshenko beam in the usual way and thus reduces the problem to a simple one. By using the present method, only standard linear eigenvalue equations, rather than non-linear algebraic equations, need to be solved. All the formulae are expressed in matrix form that renders the task of computer coding quite straightforward.

1. INTRODUCTION

Cracks found in structural elements have various causes. In metal structures, it could be fatigue cracks incurred under service conditions as a result of the limited fatigue strength. Or, it could be cracks due to material or mechanical defects in various kinds of machines. In concrete structures, it could be the opening of dry joints between precast elements, in particular in those segmental-constructed box–girder bridges assembled with dry joints that are favourable in tropical countries.

Knowing the dynamic behaviour of a structure with cracks is of significant importance in engineering. There are two types of problems related to this topic: the first may be called "direct problem" and the second called "inverse problem". The "direct problem" is to determine the effect of damages on the structural dynamic characteristics, while the "inverse problem" is to detect, locate and quantify the extent of the damages. In the past two decades, both the direct and the inverse problems have attracted many researchers and many relevant literatures have been published. Dimarogonas [1] presented the state-of-art review of various methods in tackling the cracked structure problem.

Although many researchers [2–12] studied the effect of damages on the structural dynamic characteristics, their studies were often limited to Euler beam. In fact, when the number and/or depths of cracks increase, behaviour of the cracked sub-segments is more like a 'thick beam', and therefore adopting the Timoshenko-beam theory is more reasonable than the Euler beam. Recently, Shifrin and Ruotolo [13] developed a method that can be used to tackle a beam with multiple cracks. However, their studies were limited to Euler beams.

Gudmunson [14] employed a theory based on the first order perturbation to study the effect of cracks, notches and other geometrical discontinuities on the eigenfrequencies of

0022-460X/01/370297 + 21 $35.00/0

slender structures. Via the Euler–Bernoulli beam theory, Christides and Barr [15] established a set of differential equations for one-dimensional cracked beams.

On the whole, the prevailing methods can be classified into two main categories. In the first category, the beam is modelled as an assembly of a number of sub-beams connected by massless rotational springs. Subsequently, the vibrational differential equations are established and then solved piecewisely [2–9, 13]. The second category falls within the regime of the finite element method [10–12, 14–18]. The former is a kind of continuous method while the latter is a kind of discrete method. Since the finite element solution is obtained through discretization, it is not unexpected that the continuous method will yield more accurate solutions. On the other hand, the continuous method has some limits and drawbacks. Firstly, its applications are usually limited to uniform beams. Secondly, the formulae are more complex and not unified. Thirdly, to obtain the natural frequencies, it usually requires a search of the roots of a non-linear algebraic equation (i.e., the determinant of an eigenmatrix). The main objectives of developing the present method are to alleviate these drawbacks but to retain the accuracy.

Conceptually, the simulation of a cracked beam is analogous to that of a beam with stepped changes of cross-sections and/or with intermediate point supports. Recently, the modified Fourier series (MFS) and the modified beam vibration functions (MBVF) were developed and have been successfully used in solving the vibrational problems of structures with stepped cross-sections and/or intermediate point supports [19–24].

In this paper, a new method is developed for computing the natural frequencies of a Timoshenko beam with an arbitrary number of transverse open cracks. The essence of this new method lies in the use of a kind of modified Fourier series that is developed specially for the analysis of a beam with arbitrary number of transverse open cracks. Unlike the conventional Fourier series, the modified series is able to approach a function with internal geometrical discontinuities effectively. Based on the present modified Fourier series, one can treat the cracked beam in the usual way (i.e., once the MFS is employed, the computational procedures will be the same as those for an uncracked beam) and thus reduces the problem to a *simple* one. As can be seen from the stiffness matrix in the frequency equation (63), the extra effort needed is just to add the $\mathbf{K}_4$ matrix to the stiffness matrix of the beam. In the present method, only standard linear eigenvalue equations, rather than non-linear algebraic equations, need to be solved. Since this new method falls within the frame of continuous methods, its capability of achieving higher accuracy is expected. Moreover, all the formulae are expressed in a unified way and in matrix form, which renders the computer coding quite straightforward. To demonstrate the effectiveness and accurateness of the present method, several numerical examples are shown.

2. THEORY AND FORMULATION

2.1. MODIFIED FOURIER SERIES $Y_m(y)$

Figure 1 shows a beam having $(Q-1)$ number of transverse open cracks located at $y = y_2,\ y_3, \ldots, y_Q$ and having N_0 point-spring supports located at $y = s_1,\ s_2, \ldots, s_{N_0}$ respectively. The beam can have non-uniform cross-sectional areas $A(y)$ and various second moment of area $I(y)$ along the longitudinal direction y. The depths of the cracks are $\{a_i,\ i = 1,\ 2, \ldots, Q-1\},\ a_i \geqslant 0$, and the translational and rotational stiffness of the point springs are $\{k_i, \chi_i, i = 1, 2, \ldots, N_0\}$. The point springs are introduced here for the purpose of modelling the boundary supports and the intermediate point supports, if any.

The transverse deflection and the rotation of cross-section of the Timoshenko beam are denoted by $w(y, t)$ and $\psi(y, t)$, respectively, where y stands for the location and t stands for

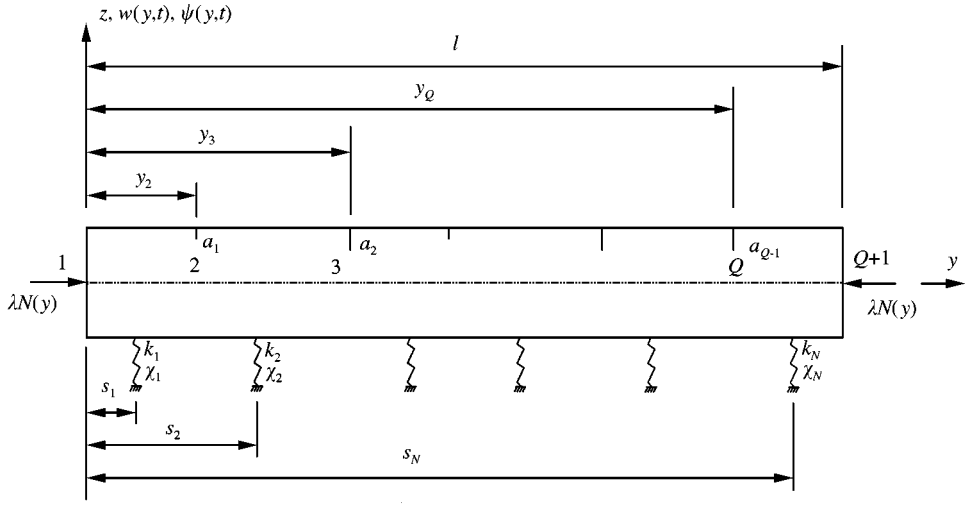

Figure 1. An axially compressed Timoshenko beam having $(Q-1)$ number of cracks located at $y = y_2$, $y_3, \ldots, y_Q$ and N spring supports located at $y = s_1, s_2, \ldots, s_N$.

the time. Considering the continuity of function $w(y, t)$ and discontinuity of function $\psi(y, t)$, we can express them as follows:

$$w(y,t) = \sum_{m=1}^{R} w_m(t)\, \bar{Y}_m(y) = \bar{\mathbf{H}}(y)\mathbf{q}_1(t) \quad (R = 2r+1), \tag{1}$$

$$\psi(y,t) = \sum_{m=1}^{R} \psi_m(t)\, Y_m(y) = \mathbf{H}(y)\mathbf{q}_2(t) \quad (R = 2r+1), \tag{2}$$

where

$$\bar{\mathbf{H}}(y) = [\bar{Y}_1(y) \quad \bar{Y}_2(y) \cdots \bar{Y}_R(y)], \tag{3}$$

$$\mathbf{H}(y) = [Y_1(y) \quad Y_2(y) \cdots Y_R(y)], \tag{4}$$

$$\mathbf{q}_1(t) = [w_1(t)\ w_2(t) \cdots w_R(t)]^{\mathrm{T}}, \tag{5}$$

$$\mathbf{q}_2(t) = [\psi_1(t)\ \psi_2(t) \cdots \psi_R(t)]^{\mathrm{T}}. \tag{6}$$

In the above equations, $w_m(t)$ and $\psi_m(t)$ are the generalized co-ordinates of deformation for the beam; $\bar{Y}_m(y)$ is the Fourier series base function [25] and $Y_m(y)$ is the so-called modified Fourier function which is specifically constructed such that it can approach a function with internal discontinuities.

In the present formulation, $Y_m(y)$ is expressed as the sum of Fourier series base function $\bar{Y}_m(y)$ and an augmenting piecewise constant function $\tilde{Y}_m(y)$ as follows:

$$Y_m(y) = \bar{Y}_m(y) + \tilde{Y}_m(y), \tag{7}$$

$$\bar{Y}_m(y) = \begin{cases} 1 & m = 1, \\ \cos(k\omega_0 y), & m = 2k;\ k = 1, 2, \ldots, r, \\ \sin(k\omega_0 y), & m = 2k+1;\ k = 1, 2, \ldots, r, \end{cases} \tag{8}$$

$$\tilde{Y}_m(y) = \sum_{j=1}^{Q} f_j l_j(y), \tag{9}$$

where $\omega_0 = \pi/l$ is the basic frequency and $l_j(y)$ are the piecewise constant interpolation base functions

$$l_j(y) = \begin{cases} 1, & y \in (y_j, y_{j+1}) \\ 0, & \text{others} \end{cases} \quad (j = 1, 2, \ldots, Q). \tag{10}$$

By adding the piecewise constant functions $\{\tilde{Y}_m(y), m = 1, 2, \ldots, R\}$ (see Figure 2) onto the basic Fourier series $\{\bar{Y}_m(y),\ m = 1,\ 2, \ldots, R\}$, we can *force* the whole function $\{Y_m(y), m = 1, 2, \ldots, R\}$ to satisfy the geometrical discontinuity conditions at the locations of cracks. Thus in the following analysis, we can treat the cracked beam in the usual way and need not further bother about the internal geometrical discontinuities.
Denoting

$$\tilde{\mathbf{H}}(y) = [\tilde{Y}_1(y)\ \ \tilde{Y}_2(y) \cdots \tilde{Y}_R(y)], \tag{11}$$

we have

$$\mathbf{H}(y) = \bar{\mathbf{H}}(y) + \tilde{\mathbf{H}}(y). \tag{12}$$

The geometrical discontinuity condition at the cracks' location $y = y_j$ ($j = 2, 3, \ldots, Q$) is [18]

$$Y_m(y_j + 0) - Y_m(y_j - 0) = c_{j-1} Y'_m(y \to y_j), \tag{13}$$

where c_{j-1} is the flexibility coefficient of the crack having a depth of a_{j-1}. For one-sided cracks, it can be expressed as

$$c_{j-1} = 5{\cdot}346h(y_j)g(\xi_{j-1}) \quad (j = 2, 3,, \ldots, Q), \tag{14}$$

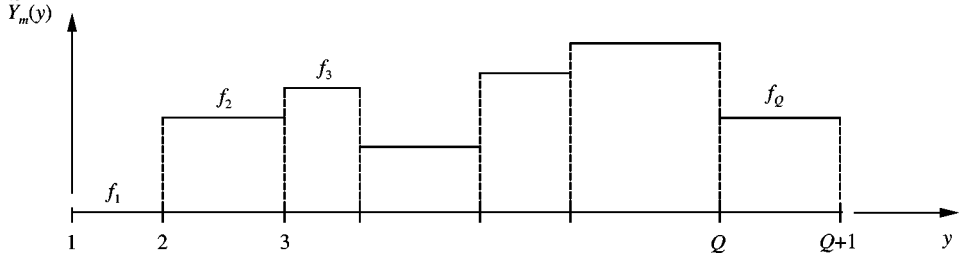

Figure 2. Augmenting piecewise constant function $\tilde{Y}_m(y)$.

where $h(y_j)$ is the depth of the cross-section of the beam at $y = y_j$ and

$$\xi_{j-1} = a_{j-1}/h(y_j), \tag{15}$$

$$g(\xi) = 1{\cdot}8624\xi^2 - 3{\cdot}95\xi^3 + 16{\cdot}375\xi^4 - 37{\cdot}226\xi^5 + 76{\cdot}81\xi^6 - 126{\cdot}9\xi^7 + 172\xi^8 - 143{\cdot}97\xi^9 + 66{\cdot}56\xi^{10}. \tag{16}$$

Substituting equation (7) into equation (13) and considering that $\bar{Y}_m(y)$ is a smooth harmonic function, we have

$$\tilde{Y}_m(y_j + 0) - \tilde{Y}_m(y_j - 0) = c_{j-1}\bar{Y}'_m(y_j). \tag{17}$$

Equation (17) can also be expressed as

$$\tilde{\mathbf{H}}(y_j + 0) - \tilde{\mathbf{H}}(y_j - 0) = c_{j-1}\bar{\mathbf{H}}'(y_j). \tag{18}$$

Substituting equations (9) and (10) into equation (17), we have

$$-f_{j-1} + f_j = c_{j-1}\bar{Y}'_m(y_j) \quad (j = 2, 3, \ldots, Q). \tag{19}$$

Setting

$$f_1 = 0, \tag{20}$$

we totally have Q number of equations which are sufficient to determine the Q number of unknown coefficients f_j. Equations (19) and (20) can be expressed in matrix form as follows:

$$\mathbf{Af} = \mathbf{b}, \tag{21}$$

where

$$\mathbf{A} = \begin{bmatrix} 1 & 0 & 0 & 0 & 0 & \cdots & 0 & 0 \\ -1 & 1 & 0 & 0 & 0 & \cdots & 0 & 0 \\ 0 & -1 & 1 & 0 & 0 & \cdots & 0 & 0 \\ 0 & 0 & 0 & \ddots & 0 & \cdots & 0 & 0 \\ 0 & 0 & 0 & 0 & \ddots & \cdots & 0 & \vdots \\ \vdots & \vdots & \vdots & \vdots & \vdots & \ddots & 0 & 0 \\ 0 & 0 & 0 & 0 & 0 & -1 & 1 & 0 \\ 0 & 0 & 0 & 0 & 0 & \cdots & -1 & 1 \end{bmatrix}, \tag{22}$$

$$\mathbf{f} = [f_1 \quad f_2 \quad f_3 \quad \cdots \quad \cdots \quad f_{Q-2} \quad f_{Q-1} \quad f_Q]^{\mathrm{T}}, \tag{23}$$

$$\mathbf{b} = [0 \quad c_1\bar{Y}'_m(y_2) \quad c_2\bar{Y}'_m(y_3) \quad \cdots \quad \cdots \quad \cdots \quad c_{Q-2}\bar{Y}'_m(y_{Q-1}) \quad c_{Q-1}\bar{Y}'_m(y_Q)]^{\mathrm{T}}. \tag{24}$$

By solving equation (21), we can determine the coefficients f_j ($j = 1, 2, \ldots, Q$) and thus determine the augmenting piecewise constant functions $\tilde{Y}_m(y)$ and the modified Fourier series $Y_m(y)$.

2.2. ENERGY ANALYSIS

2.2.1. *Potential energy*

The potential energy of a cracked Timoshenko beam under axial load can be expressed as the summation of the following five parts:

$$U = U_1 + U_2 + U_3 + U_4 + U_5, \tag{25}$$

in which U_1 and U_2 are the potential energy stored in the cracked beam due to bending and shearing deformation of the beam itself; U_3 is the potential energy stored in the point springs which are used to model the boundary supports and also the intermediate supports (if any); U_4 is the potential energy stored in the massless rotational springs which are used to model the existence of cracks; U_5 is the potential energy of the external variable axial load $\lambda N(y)$.

Potential energy U_1:

$$U_1 = \sum_{i=1}^{Q} \frac{1}{2} \int_{y_i}^{y_{i+1}} EI(y)\psi_{,y}^2(y,t)\,\mathrm{d}y. \tag{26}$$

Substituting equation (2) into equation (26), we have

$$U_1 = \tfrac{1}{2}\,\mathbf{q}_2^{\mathrm{T}}\mathbf{K}_1\mathbf{q}_2, \tag{27}$$

where $\mathbf{K}_1$ represents the stiffness matrix of the cracked beam corresponding to the potential energy U_1 such that

$$\mathbf{K}_1 = \sum_{i=1}^{Q} \int_{y_i}^{y_{i+1}} EI(y)\mathbf{H}_{,y}^{\mathrm{T}}(y)\,\mathbf{H}_{,y}(y)\,\mathrm{d}y = \int_0^l EI(y)\bar{\mathbf{H}}_{,y}^{\mathrm{T}}(y)\bar{\mathbf{H}}_{,y}(y)\,\mathrm{d}y. \tag{28}$$

Potential energy U_2:

$$U_2 = \frac{1}{2}\int_0^l k'GA(y)(w_{,y} - \psi)^2\,\mathrm{d}y. \tag{29}$$

Substituting equations (1) and (2) into equation (29), we have

$$U_2 = \tfrac{1}{2}\mathbf{q}_1^{\mathrm{T}}\mathbf{K}_{21}\mathbf{q}_1 - \mathbf{q}_1^{\mathrm{T}}\mathbf{K}_{22}\mathbf{q}_2 + \tfrac{1}{2}\mathbf{q}_2^{\mathrm{T}}\mathbf{K}_{23}\mathbf{q}_2, \tag{30}$$

where

$$\mathbf{K}_{21} = \int_0^l k'GA(y)\bar{\mathbf{H}}_{,y}^{\mathrm{T}}(y)\bar{\mathbf{H}}_{,y}(y)\,\mathrm{d}y, \tag{31}$$

$$\mathbf{K}_{22} = \int_0^l k'GA(y)\bar{\mathbf{H}}_{,y}^{\mathrm{T}}(y)\mathbf{H}(y)\,\mathrm{d}y, \tag{32}$$

$$\mathbf{K}_{23} = \int_0^l k'GA(y)\bar{\mathbf{H}}^{\mathrm{T}}(y)\mathbf{H}(y)\,\mathrm{d}y. \tag{33}$$

Potential energy U_3:

$$U_3 = \sum_{i=1}^{N_\theta} \frac{1}{2} [k_i w^2(s_i, t) + \chi_i \psi^2(s_i, t)]. \tag{34}$$

Substituting equations (1) and (2) into equation (34), we have

$$U_3 = \tfrac{1}{2} \mathbf{q}_1^{\mathrm{T}} \mathbf{K}_{31} \mathbf{q}_1 + \tfrac{1}{2} \mathbf{q}_2^{\mathrm{T}} \mathbf{K}_{32} \mathbf{q}_2, \tag{35}$$

where

$$\mathbf{K}_{31} = \sum_{i=1}^{N_\theta} k_i \bar{\mathbf{H}}^{\mathrm{T}}(s_i) \bar{\mathbf{H}}(s_i), \tag{36}$$

$$\mathbf{K}_{32} = \sum_{i=1}^{N_\theta} \chi_i \mathbf{H}^{\mathrm{T}}(s_i) \mathbf{H}(s_i). \tag{37}$$

Potential energy U_4:

$$U_4 = \sum_{j=2}^{Q} \frac{1}{2} \left[\frac{EI(y_j)}{c_{j-1}} \right] [\psi(y_j + 0, t) - \psi(y_j - 0, t)]^2. \tag{38}$$

Substituting equation (2) into equation (38), we have

$$U_4 = \tfrac{1}{2} \mathbf{q}_2^{\mathrm{T}} \mathbf{K}_4 \mathbf{q}_2, \tag{39}$$

where $\mathbf{K}_4$ represents the stiffness matrix of the cracked beam corresponding to the potential energy U_4 such that

$$\mathbf{K}_4 = \sum_{j=2}^{Q} [c_{j-1} EI(y_j)] \bar{\mathbf{H}}_{,y}^{\mathrm{T}}(y_j) \bar{\mathbf{H}}_{,y}(y_j). \tag{40}$$

Potential energy U_5:

$$U_5 = -\frac{1}{2} \lambda \int_0^l N(y) w_{,y}^2(y, t) \, \mathrm{d}y. \tag{41}$$

Substituting equation (1) into equation (41), we have

$$U_5 = -\tfrac{1}{2} \mathbf{q}_1^{\mathrm{T}} (\lambda \mathbf{K}_G) \mathbf{q}_1, \tag{42}$$

where $\mathbf{K}_G$ represents the stiffness matrix of the cracked beam corresponding to the potential energy U_5 such that,

$$\mathbf{K}_G = \int_0^l N(y) \bar{\mathbf{H}}_{,y}^{\mathrm{T}} \bar{\mathbf{H}}_{,y} \, \mathrm{d}y. \tag{43}$$

Finally, substituting equations (27), (30), (35) and (39) into equation (25), we obtain the total potential energy of the cracked-beam system

$$U = \tfrac{1}{2} \mathbf{q}_1^{\mathrm{T}} (\mathbf{K}_{21} + \mathbf{K}_{31} - \lambda \mathbf{K}_G) \mathbf{q}_1 + \tfrac{1}{2} \mathbf{q}_2^{\mathrm{T}} (\mathbf{K}_1 + \mathbf{K}_{23} + \mathbf{K}_{32} + \mathbf{K}_4) \mathbf{q}_2 - \mathbf{q}_1^{\mathrm{T}} \mathbf{K}_{22} \mathbf{q}_2. \tag{44}$$

2.2.2. *Kinetic energy*

The kinetic energy of the Timoshenko beam can be expressed as the summation of the two parts, T_1 and T_2, such that

$$T = T_1 + T_2, \tag{45}$$

in which T_1 and T_2 are the kinetic energy stored in the Timoshenko beam due to translational and rotational deformation respectively.

The translational kinetic energy T_1 of the Timoshenko beam can be expressed as

$$T_1 = \frac{1}{2}\int_0^l \rho A(y) w_{,t}^2(y, t)\,\mathrm{d}y. \tag{46}$$

Substituting equation (1) into equation (46), we have

$$T_1 = \tfrac{1}{2}\dot{\mathbf{q}}_1^{\mathrm{T}}\mathbf{M}_1\dot{\mathbf{q}}_1, \tag{47}$$

where

$$\mathbf{M}_1 = \int_0^l \rho A(y)\bar{\mathbf{H}}^{\mathrm{T}}(y)\bar{\mathbf{H}}(y)\mathrm{d}y. \tag{48}$$

The rotational kinetic energy T_2 of the Timoshenko beam can be expressed as

$$T_2 = \frac{1}{2}\int_0^l J(y)\psi_{,t}^2(y, t)\,\mathrm{d}y. \tag{49}$$

Substituting equation (2) into equation (49), we have

$$T_2 = \tfrac{1}{2}\dot{\mathbf{q}}_2^{\mathrm{T}}\mathbf{M}_2\dot{\mathbf{q}}_2, \tag{50}$$

where

$$\mathbf{M}_2 = \int_0^l J(y)\mathbf{H}^{\mathrm{T}}(y)\mathbf{H}(y)\,\mathrm{d}y. \tag{51}$$

Finally, substituting equations (47) and (50) into equation (45), we obtain the total kinetic energy of the Timoshenko beam,

$$T = \tfrac{1}{2}\dot{\mathbf{q}}_1^{\mathrm{T}}\mathbf{M}_1\dot{\mathbf{q}}_1 + \tfrac{1}{2}\dot{\mathbf{q}}_2^{\mathrm{T}}\mathbf{M}_2\dot{\mathbf{q}}_2. \tag{52}$$

2.3. EULER–LAGRANGIAN EQUATIONS

The Euler–Lagrangian equations of the cracked Timoshenko beam are

$$\frac{\mathrm{d}}{\mathrm{d}t}\left(\frac{\partial L}{\partial \dot{\mathbf{q}}_1}\right) - \frac{\partial L}{\partial \mathbf{q}_1} = \mathbf{0}, \quad \frac{\mathrm{d}}{\mathrm{d}t}\left(\frac{\partial L}{\partial \dot{\mathbf{q}}_2}\right) - \frac{\partial L}{\partial \mathbf{q}_2} = \mathbf{0}, \tag{53, 54}$$

where L is the Lagrangian function such that

$$L = T - U. \tag{55}$$

Substituting equations (52) and (44) into equation (55), and then the results into equations (53) and (54), we have

$$\mathbf{M}_1\ddot{\mathbf{q}}_1 + (\mathbf{K}_{21} + \mathbf{K}_{31} - \lambda\mathbf{K}_G)\mathbf{q}_1 - \mathbf{K}_{22}\mathbf{q}_2 = \mathbf{0}, \tag{56}$$

$$\mathbf{M}_2\ddot{\mathbf{q}}_2 + (\mathbf{K}_1 + \mathbf{K}_{23} + \mathbf{K}_{32} + \mathbf{K}_4)\mathbf{q}_2 - \mathbf{K}_{22}^{\mathrm{T}}\mathbf{q}_1 = \mathbf{0}. \tag{57}$$

Equations (56) and (57) can be written into one matrix equation

$$\mathbf{M}\ddot{\mathbf{q}} + \mathbf{K}\mathbf{q} = \mathbf{0}, \tag{58}$$

where

$$\mathbf{M} = \begin{bmatrix} \mathbf{M}_1 & \mathbf{0} \\ \mathbf{0} & \mathbf{M}_2 \end{bmatrix}, \tag{59}$$

$$\mathbf{K} = \begin{bmatrix} \mathbf{K}_{21} + \mathbf{K}_{31} - \lambda\mathbf{K}_G & -\mathbf{K}_{22} \\ -\mathbf{K}_{22}^{\mathrm{T}} & \mathbf{K}_1 + \mathbf{K}_{23} + \mathbf{K}_{32} + \mathbf{K}_4 \end{bmatrix}, \tag{60}$$

$$\mathbf{q} = \begin{bmatrix} \mathbf{q}_1 \\ \mathbf{q}_2 \end{bmatrix}. \tag{61}$$

2.4. FREQUENCY EQUATION

For synchronous vibration, we have

$$\mathbf{q}(t) = \mathbf{q}\cos(\omega t + \phi). \tag{62}$$

Substituting equation (62) into equation (58), we can obtain the frequency equation

$$\mathbf{K}\mathbf{q} = \omega^2\mathbf{M}\mathbf{q}. \tag{63}$$

Equation (63) is a standard linear eigenvalue equation that can be solved by standard programs. It is worth noting that the matrix $\mathbf{K}_4$ represents the additional stiffness contributed from the massless rotational springs, which are used to model the cracks in the beam. However, contrary to the conventional belief that higher stiffness will lead to increase of vibration frequencies, the presence of crack(s) will result in the overall reduction of vibration frequencies. This physical phenomenon is taken into account in the mathematical representation in the present method by using the modified Fourier series, which is discontinuous at the crack locations.

3. NUMERICAL EXAMPLES

Several numerical examples are shown in this section. It is worth noting that, for modelling the boundary conditions, we use very big (10^{10}–10^{14}) translational and rotational

stiffness of the springs (i.e., κ_i and χ_i) in the numerical computations. In the following examples, the order of the highest harmonic r adopted is in the range of 5–12 to achieve converged results.

3.1. EXAMPLE 1: A CANTILEVERED THICK AND THIN BEAM WITH AND WITHOUT CRACKS

To validate the present theory and the computer coding, firstly the natural frequencies of a *thick* cantilevered beam and a *thin* cantilevered beam without cracks were computed and the results were compared with those in references [26, 27]. The cantilevered beam has the geometrical properties: length l; square cross-section (i.e., width b equals height h). Same parameters as those in references [26, 27] were used: the depth-to-span ratio equals 0·1 for a thick beam and 0·001 for a thin beam, respectively; the cross-section coefficient k' equals 0·822. The dimensionless frequencies $\Omega_j = ((l^2/h)\sqrt{2(1+\mu)\rho/E})\omega_j$ are presented. Two

TABLE 1

Values of Ω for thick and thin CF beams

	$h/L = 0{\cdot}1$			$h/L = 0{\cdot}001$		
	Ω_1	Ω_2	Ω_3	Ω_1	Ω_2	Ω_3
Present	1·6236	9·7266	25·5684	1·6366	10·2564	28·7181
Dawe and Wang [26]	1·6236	9·7266	25·568	1·6366	10·256	28·718
Wang [27]	1·6236	9·7268	25·578	1·6366	10·256	28·720

TABLE 2

Values of Ω for thick and thin CC beams

	$h/L = 0{\cdot}1$			$h/L = 0{\cdot}001$		
	Ω_1	Ω_2	Ω_3	Ω_1	Ω_2	Ω_3
Present	9·7545	25·9810	45·1226	10·4141	28·7067	56·2758
Dawe and Wang [26]	9·7545	24·981	45·123	10·414	28·707	56·276
Wang [27]	9·7546	24·987	45·201	10·414	28·708	56·304

TABLE 3

Natural frequencies of a cracked Timoshenko beam

Natural frequency	Cracked beam			Uncracked beam
	Present	Kisa *et al.* [28]	Error (%)	Kisa *et al.* [28]
ω_1	1024·963	1020·137	0·5	1037·019
ω_2	6441·290	6457·396	0·2	6458·344
ω_3	17737·870	17872·91	0·8	17960·564

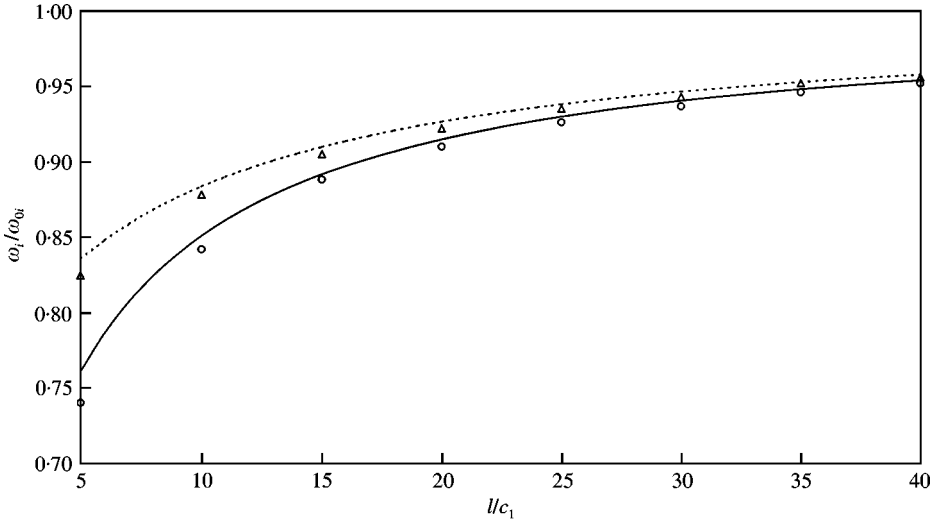

Figure 3. Effect of a single crack at clamped end on natural frequencies of a beam: ——, first freq. (Timoshenko beam, present); ○, first freq. (Euler beam [13]); - - - -, second freq. (Timoshenko beam, present); △, second freq. (Euler beam [13]).

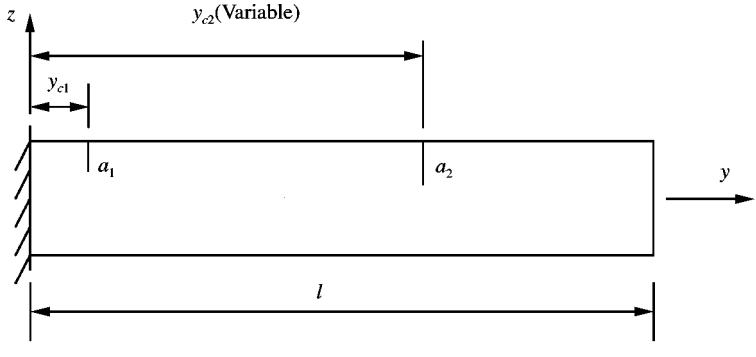

Figure 4. A cantilevered beam with two cracks while the second crack's location is variable.

cases are considered. One is clamped–free (CF) and another is clamped–clamped (CC). The first three frequencies obtained by the present method are compared with those in references [26, 27] as shown in Tables 1 and 2. Perfect agreement is observed.

Subsequently, the results for a cracked Timoshenko beam were computed and compared with those in reference [28]. Again, same parameters as those in reference [28] were used: $l = 0{\cdot}2$ m, $b = 0{\cdot}025$ m, $h = 0{\cdot}0078$ m, $E = 216$ GPa, $\mu = 0{\cdot}28$ and $\rho = 7850$ kg/m^3. The crack is located at $\xi = 0{\cdot}2l$ and the crack depth is $a = 0{\cdot}2h$. The first three natural frequencies obtained from the present method are compared with those in reference [28] as shown in Table 3. Again, excellent agreement is observed.

It can be seen from Table 3 that higher order modes exhibit less reduction in frequency than lower order modes do.

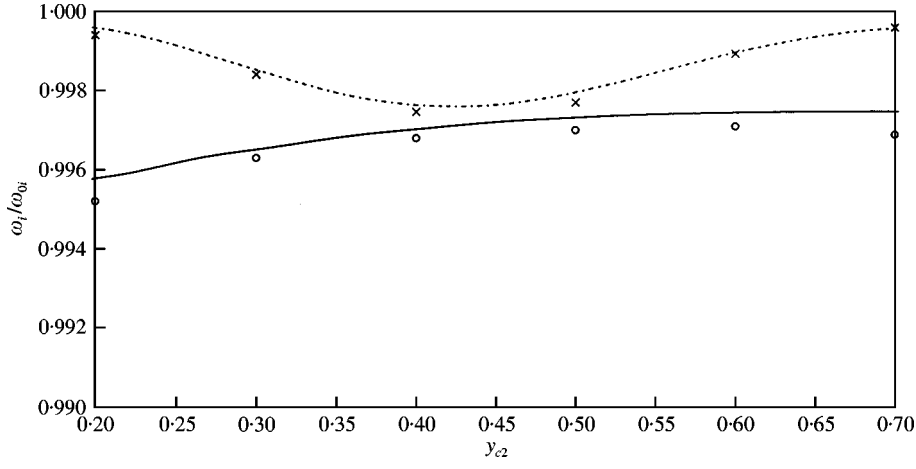

Figure 5. Effect of locations of a second crack ($a_2 = 2$ mm) on natural frequencies of a beam: ——, first freq. (Timoshenko beam, present); ○, first freq. (Euler beam [13]); - - - -, second freq. (Timoshenko beam, present); ×, second freq. (Euler beam [13]).

3.2. EXAMPLE 2: A CANTILEVERED BEAM WITH A CRACK LOCATED AT THE CLAMPED END [13]

Consider a cantilevered beam with a crack located at the clamped end. The results obtained by the present method and the results from reference [13] are shown in Figure 3. In Figure 3, the vertical axis stands for the frequency ratio of the natural frequencies of the cracked beam to the natural frequencies of the same but uncracked beam, i.e., the frequency reduction. The horizontal axis stands for the normalized stiffness (l/c_1) of the artificial rotational spring introduced at the crack. It can be seen that the frequency reduction of a Timoshenko beam is less than that of a Euler beam [13]. This is not surprising because Timoshenko beam is less stiff than a Euler beam. Therefore, Timoshenko beam is less sensitive to the cracks. It is worth nothing that the differences in frequency reductions between the Euler- and the Timoshenko-beam model diminished when the depths of cracks are very small (i.e., when l/c_1 is large).

3.3. EXAMPLE 3: A CANTILEVERED BEAM WITH TWO CRACKS [13]

Figure 4 shows a cantilevered beam with two cracks. For the purpose of comparing the results from reference [13], the same geometrical properties of the beam are used, i.e., length $l = 0{\cdot}8$ m; rectangular cross-section having width $b = 0{\cdot}02$ m and height $h = 0{\cdot}02$ m. The first crack is at a fixed location $y_{c1} = 0{\cdot}12$ m and has a depth $a_1 = 2$ mm. The second crack's location varies from the left end to the right end of the beam and its depth also varies ($a_2 = 2$ or 4 or 6 mm). The results obtained by the present method and those from reference [13] are shown in Figures 5–7. It can be seen from Figures 5–7 that the thicker the crack goes, the bigger is the difference in frequency reduction between the Timoshenko- and the Euler-beam model. In fact, when more cracks or deeper cracks occur in a beam, the beam tends to behave more like "thick beams" because the effect of shear deformation becomes more significant.

3.4. EXAMPLE 4: A THICK CANTILEVERED BEAM WITH TWO CRACKS

In order to illustrate the effect of shear deformation, which is taken into account in the Timoshenko beam, a thick cantilevered beam with two cracks is studied (as shown in

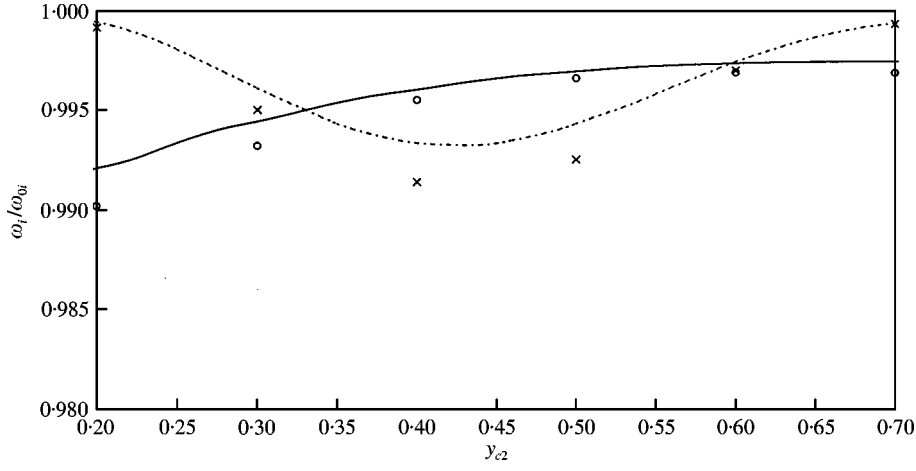

Figure 6. Effect of locations of a second crack ($a_2 = 4$ mm) on natural frequencies of a beam: ——, first freq. (Timoshenko beam, present); ○, first freq. (Euler beam [13]); - - - -, second freq. (Timoshenko beam, present); ×, second freq. (Euler beam [13]).

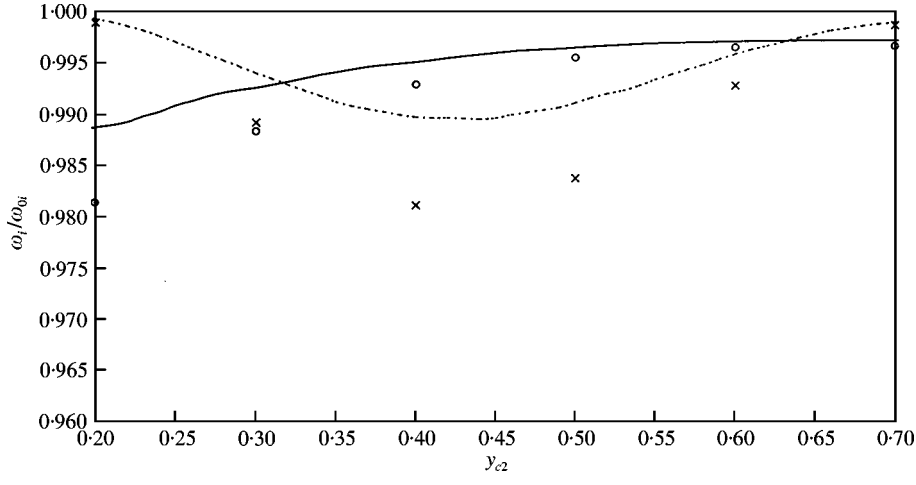

Figure 7. Effect of locations of a second crack ($a_2 = 6$ mm) on natural frequencies of a beam: ——, first freq. (Timoshenko beam, present); ○, first freq. (Euler beam [13]); - - - -, second freq. (Timoshenko beam, present); ×, second freq. (Euler beam [13]).

Figure 4). The beam has the geometrical properties: length $l = 0{\cdot}8$ m, rectangular cross-section having width $b = 0{\cdot}1$ m and height $h = 0{\cdot}2$ m. The first crack is at a fixed location $y_{c1} = 0{\cdot}12$ m and has a depth $a_1 = 30$ mm. The results are shown in Figures 8–10. The same trend can be seen from Figures 8–10 that the deeper the crack goes, the bigger is the difference in frequency reduction between the Timoshenko- and the Euler-beam model. Besides, the effect of shear deformation and rotation become very significant, in particular for higher order frequencies.

3.5. EXAMPLE 5: A TWO-SPAN CONTINUOUS GIRDER WITH TWO "CRACKS"

Figure 11 shows a two-span continuous girder built by segmental construction method. The total length (1) of the bridge is $2 \times 33 = 66$ mm, composed of $2 \times 10 = 20$ segments. The

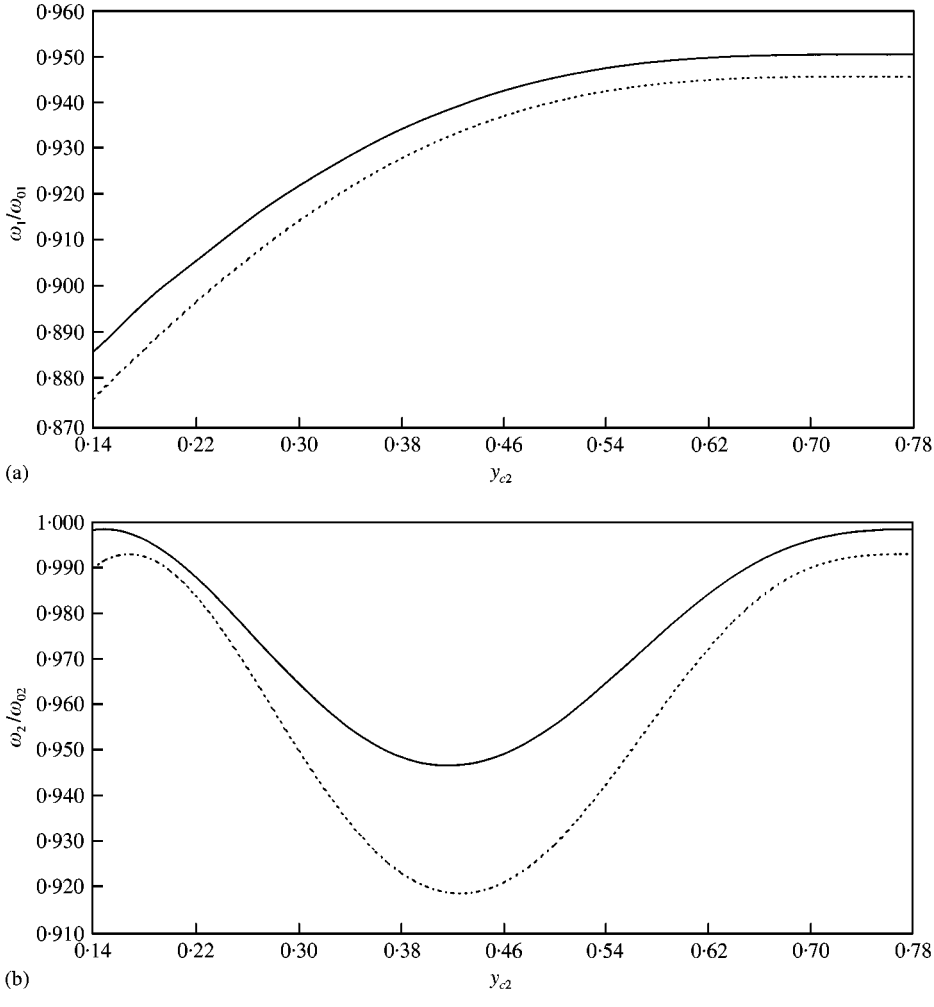

Figure 8. (a) Effect of locations of a second crack ($a_2 = 0{\cdot}04$ m) on the first natural frequency of a thick beam: ——, Timoshenko beam (present); - - - -, Euler beam [29]. (b) Effect of locations of a second crack ($a_2 = 0{\cdot}04$ m) on the second natural frequency of a thick beam: ——, Timoshenko beam (present); - - - -, Euler beam [29].

20 segments are held together via longitudinal pre-stressing force. Joints between segments are dry joints (i.e., no cement mortar). It has a constant cross-sectional area $A = 1{\cdot}9892\ \text{m}^2$, second moment of area $I = 0{\cdot}8804\ \text{m}^4$, and depth $h = 1{\cdot}9$ m. The pre-stressing force is an axial force $F = 10$ MN without eccentricity from the centroidal axis. Young's modulus is taken as 20 GPa and the Poisson ratio is 0·2. The first crack's location varies from the leftmost segment joint to the rightmost segment joint in the left span and the depth varies ($a_1 = 0{\cdot}25$, 0·5 and 0·75 m). The second crack is sited at a fixed location in the mid-span of

Figure 9. (a) Effect of locations of a second crack ($a_2 = 0{\cdot}08$ m) on the first natural frequency of a thick beam: ——, Timoshenko beam (present); - - - -, Euler beam [29]. (b) Effect of locations of a second crack ($a_2 = 0{\cdot}08$ m) on the second natural frequency of a thick beam: ——, Timoshenko beam (present); - - - -, Euler beam [29]. (c) Effect of locations of a second crack ($a_2 = 0{\cdot}08$ m) on the third natural frequency of a thick beam: ——, Timoshenko beam (present); - - - -, Euler beam.

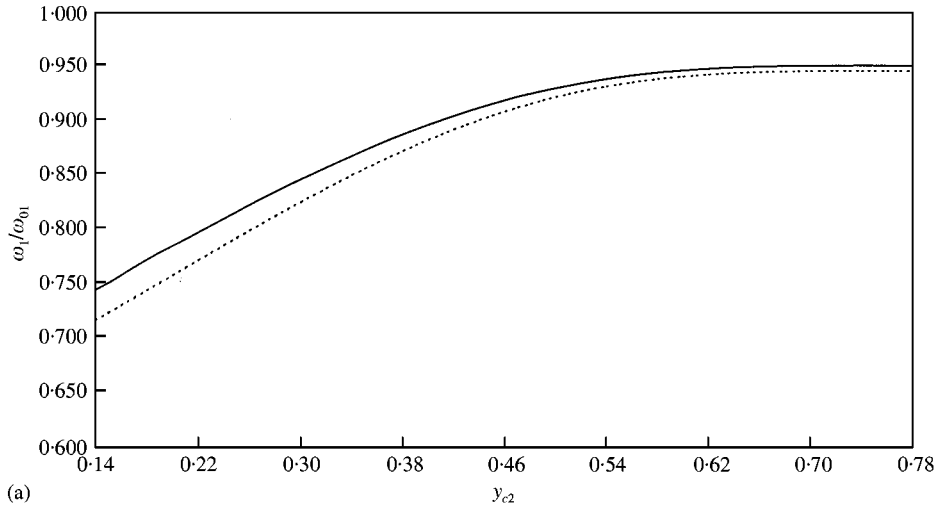
1·000
0·950
0·900
0·850
0·800
0·750
0·700
0·650
0·600
ω_1/ω_{01}
0·14
0·22
0·30
0·38
0·46
0·54
0·62
0·70
0·78
y_{c2}

(a)

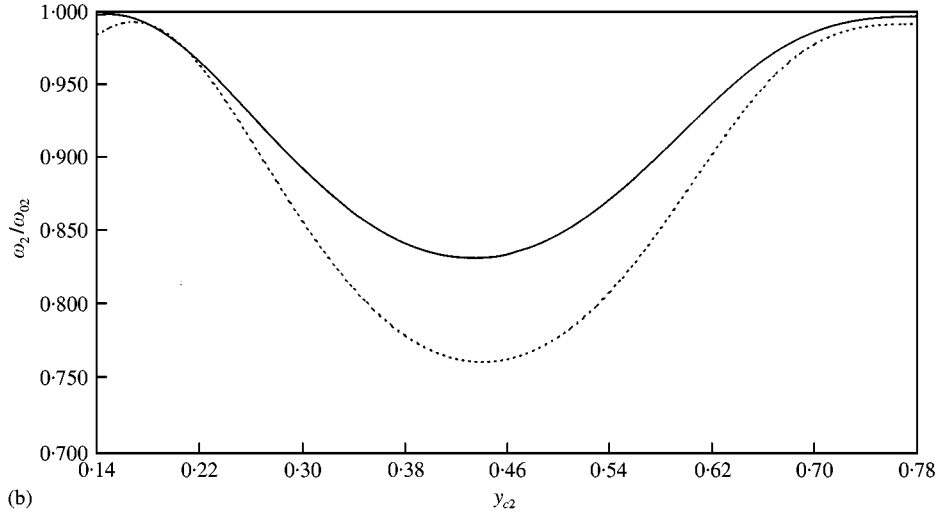
1·000
0·950
0·900
0·850
0·800
0·750
0·700
ω_2/ω_{02}
0·14
0·22
0·30
0·38
0·46
0·54
0·62
0·70
0·78
y_{c2}

(b)

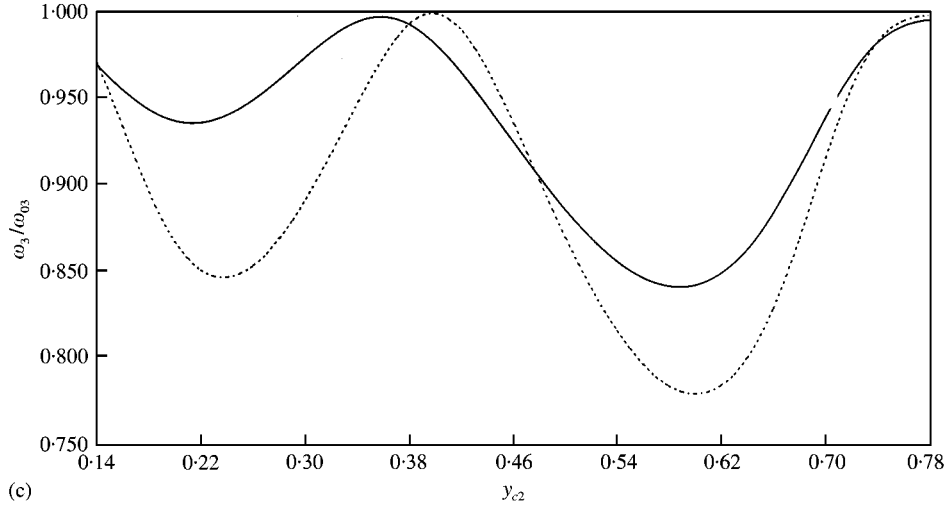
1·000
0·950
0·900
0·850
0·800
0·750
ω_3/ω_{03}
0·14
0·22
0·30
0·38
0·46
0·54
0·62
0·70
0·78
y_{c2}

(c)

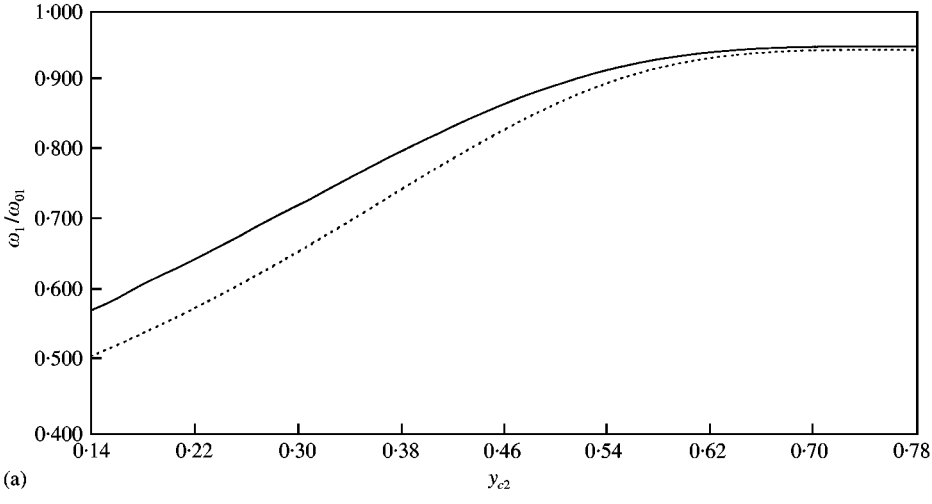
1·000
0·900
0·800
0·700
0·600
0·500
0·400
ω_1/ω_{01}
0·14
0·22
0·30
0·38
0·46
0·54
0·62
0·70
0·78
y_{c2}

(a)

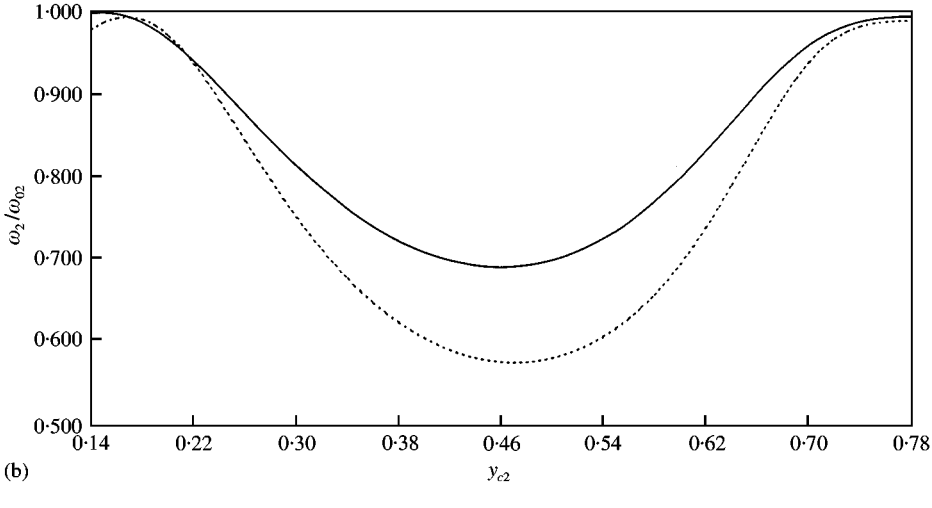
1·000
0·900
0·800
0·700
0·600
0·500
ω_2/ω_{02}
0·14
0·22
0·30
0·38
0·46
0·54
0·62
0·70
0·78
y_{c2}

(b)

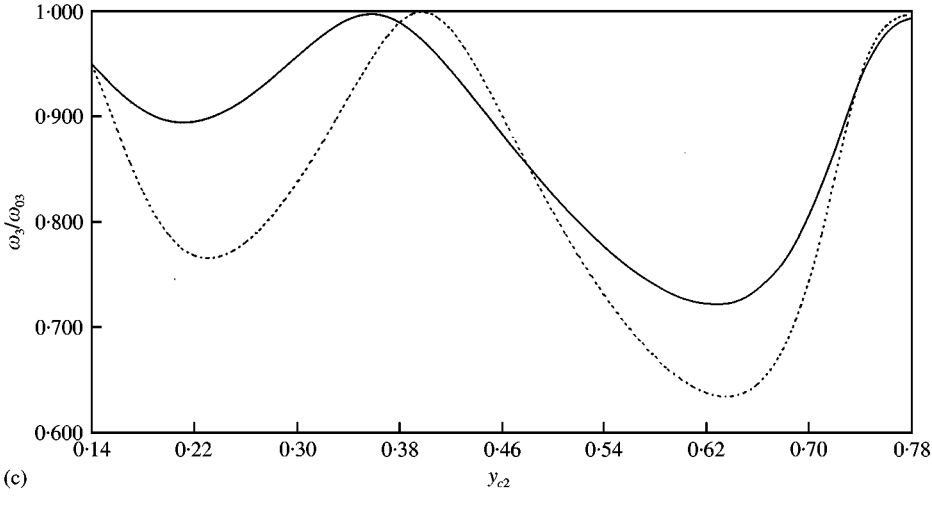
1·000
0·900
0·800
0·700
0·600
ω_3/ω_{03}
0·14
0·22
0·30
0·38
0·46
0·54
0·62
0·70
0·78
y_{c2}

(c)

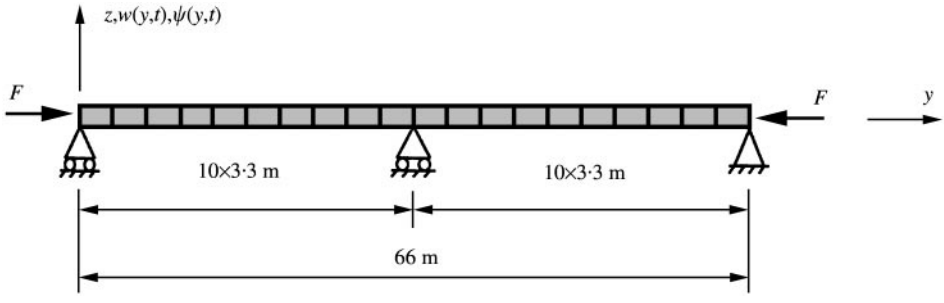

Figure 11. A two-span segmental box–girder–bridge.

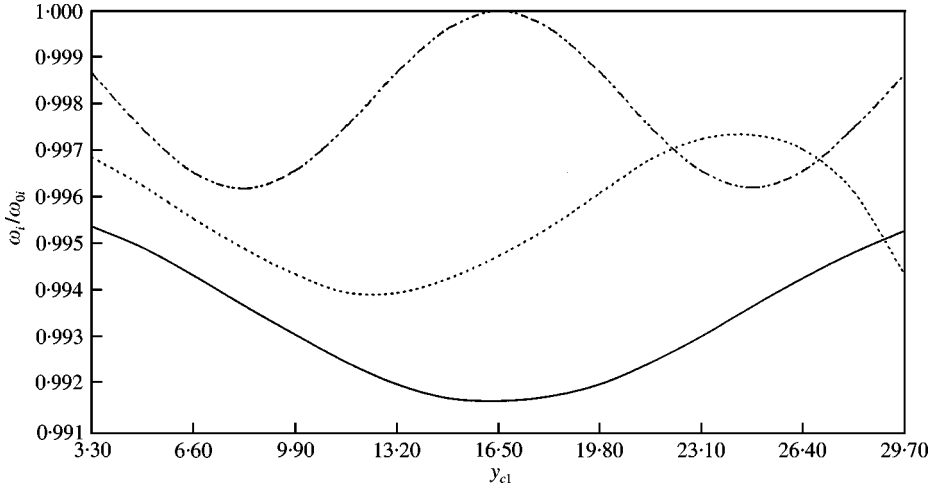

Figure 12. Effect of locations of a "crack" ($a_1 = 0{\cdot}25$ m) on natural frequencies of a two-span continuous girder: ——, first freq.; - - - -, second freq.; – – –, third freq.

the right span ($y_{c2} = 49{\cdot}5$ m) and has a fixed depth $a_2 = 0{\cdot}25$ m. The results are shown in Figures 12–14, which show the effect of the unexpected opening of dry joints on the natural frequencies of the segmental girder. Figures 12–14 suggest that by detecting the change of the natural frequencies of the girder, one can monitor the opening of the dry joints.

4. CONCLUSIONS

A new modified Fourier series (MFS) was presented. It was developed to tackle the problem in beams with arbitrary number of cracks. The modified Fourier series can

←

Figure 10. (a) Effect of locations of a second crack ($a_2 = 0{\cdot}12$ m) on the first natural frequency of a thick beam: ——, Timoshenko beam (present); - - - -, Euler beam [29]. (b) Effect of locations of a second crack ($a_2 = 0{\cdot}12$ m) on the second natural frequency of a thick beam: ——, Timoshenko beam (present); - - - -, Euler beam [29]. (c) Effect of locations of a second crack ($a_2 = 0{\cdot}12$ m) on the third natural frequency of a thick beam: ——, Timoshenko beam (present); - - - -, Euler beam [29].

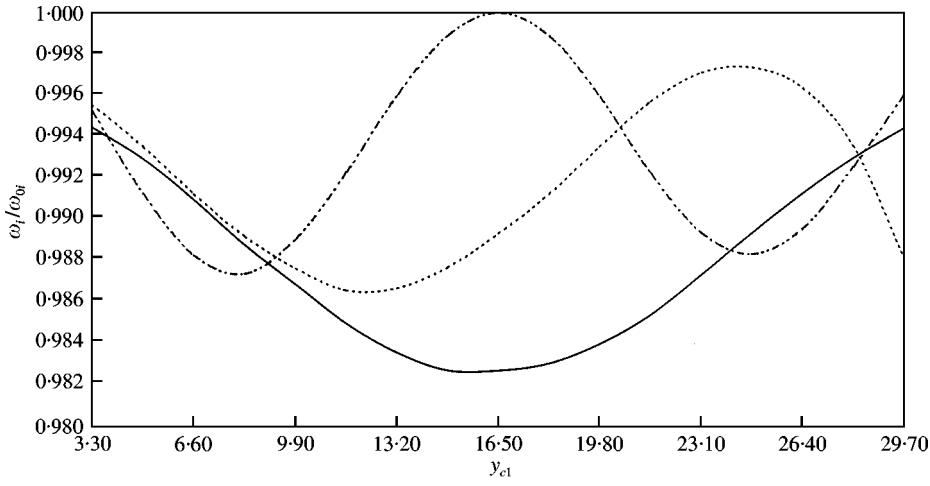

Figure 13. Effect of locations of a "crack" ($a_1 = 0{\cdot}5$ m) on natural frequencies of a two-span continuous girder: ——, first freq.; - - - -, second freq.; – – –, third freq.

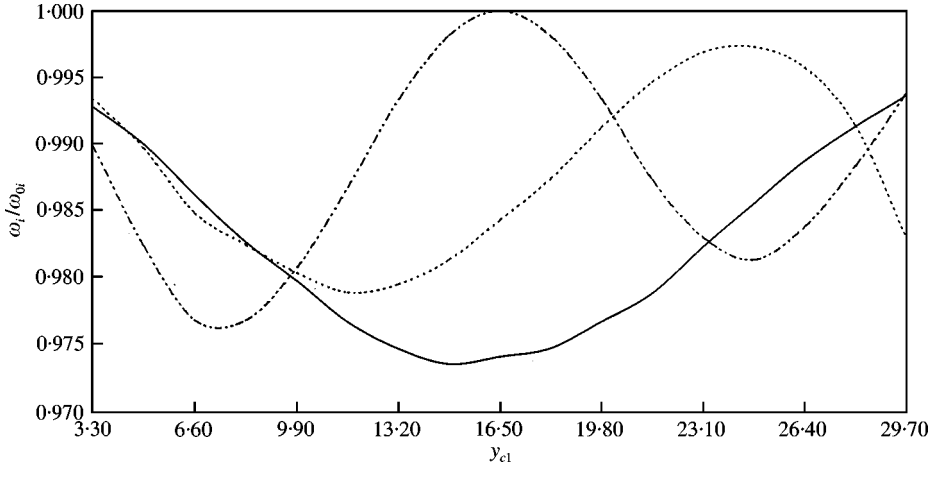

Figure 14. Effect of locations of a "crack" ($a_1 = 0{\cdot}75$ m) on natural frequencies of a two-span continuous girder: ——, first freq.; - - - -, second freq.; – – –, third freq.

approach a function with internal geometrical discontinuities effectively. Via the Euler–Lagrangian equation, we can treat the vibrational analysis of a cracked beam in the usual way. It thus renders the problem-solving procedures simple. In the formulation, an open crack is assumed as having stiffness, which is simply added to the stiffness matrix of the beam. The beam can be of non-uniform cross-section and the number of cracks can be arbitrary. In solving the natural frequencies of a cracked beam, only a standard linear eigenvalue equation needs to be solved. All the formulae are expressed in matrix form and therefore computer coding is straightforward. Numerical examples showed that the present method is versatile and effective.

REFERENCES

1. A. D. DIMAROGONAS 1996 *Engineering Fracture Mechanics* **55**, 831–857. Vibration of cracked structures: a state of the art review.
2. P. F. RIZOS, N. ASPRAGATOS and A. D. DIMAROGONAS 1990 *Journal of Sound and Vibration* **138**, 381–388. Identification of crack location and magnitude in a cantilever beam from the vibration modes.
3. W. M. OSTACHOWICZ and M. KRAWCZUK 1991 *Journal of Sound and Vibration* **150**, 191–201. Analysis of the effect of cracks on the natural frequencies of a cantilever beam.
4. R. RUOTOLO, C. SURACE and C. MARES 1996 *Proceedings of* 14th *International Modal Analysis Conference*, 1560–1564. Theoretical and experimental study of the dynamic behaviour of a double-cracked beam.
5. T. G. CHONDROS and A. D. DIMAROGONAS 1980 *Journal of Sound and Vibration* **69**, 531–538. Identification of cracks in welded joints of complex structures.
6. R. Y. LIANG, J. HU and F. CHOY 1992 *Journal of Engineering Mechanics* **118**, 384–396. Theoretical study of crack-induced eigenfrequency changes on beam structures.
7. R. Y. LIANG, J. HU and F. CHOY 1992 *Journal of Engineering Mechanics* **118**, 1468–1487. Quantitative NDE techniques for assessing damages in beam structures.
8. R. Y. LIANG, F. CHOY and J. HU 1991 *Journal of the Franklin Institute* **328**, 505–518. Detection of cracks in beam structures using measurements of natural frequencies.
9. J. HU and R. Y. LIANG 1993 *Journal of the Franklin Institute* **330**, 841–853. An integrated approach to detection of cracks using vibration characteristics.
10. G. L. QIAN, S. N. GU and J. S. JIANG 1990 *Journal of Sound and Vibration* **138**, 233–243. The dynamic behaviour and crack detection of a beam with a crack.
11. Y. NARKIS 1993 *Journal of Sound and Vibration* **172**, 549–558. Identification of cracks' location in vibrating simply supported beams.
12. A. MORASSI 1993 *Journal of Engineering Mechanics* **119**, 1768–1803. Crack-induced changes in eigenfrequencies of beam structures.
13. E. I. SHIFRIN and R. RUOTOLO 1999 *Journal of Sound and Vibration* **222**, 409–423. Natural frequencies of a beam with an arbitrary number of cracks.
14. P. GUDMUNSON 1983 *Journal of Mechanics and Physics of Solids* **31**, 329–345. The dynamic behaviour of slender structures with cross-sectional cracks.
15. S. CHRISTIDES and A. D. S. BARR 1984 *International Journal of Mechanical Science* **26**, 639–648. One-dimensional theory of cracked Euler–Bernoulli beams.
16. G. GOUNARIS and A. D. DIMAROGONAS 1988 *Computers and Structures* **28**, 309–313. A finite element of a cracked prismatic beam for structural analysis.
17. T. Y. KAM and T. Y. LEE 1992 *Engineering Fracture Mechanics* **42**, 381–387. Detection of cracks in structures using modal test data.
18. B. S. HARISTY and W. T. SPRINGER 1988 *Journal of Vibration, Acoustics, Stress and Reliability in Design* **110**, 389–394. A general beam element for use in damage assessment of complex structures.
19. D. Y. ZHENG, Y. K. CHEUNG, F. T. K. AU and Y. S. CHENG 1998 *Journal of Sound and Vibration* **212**, 455–467. Vibration of multi-span non-uniform beams under moving loads by using modified beam vibration functions.
20. F. T. K. AU, D. Y. ZHENG and Y. K. CHEUNG 1999 *Applied Mathematical Modeling* **29**, 19–34. Vibration and stability of non-uniform beams with abrupt changes of cross-section by using C^1 modified beam vibration functions.
21. Y. K. CHEUNG, F. T. K. AU and D. Y. ZHENG 1998 *Thin Walled Structures* **32**, 289–303. Analysis of deep beams and shear walls by finite strip method with C^0 continuous displacement functions.
22. Y. K. CHEUNG, F. T. K. AU, D. Y. ZHENG and Y. S. CHENG 1999 *Journal of Sound and Vibration* **228**, 611–628. Vibration of multi-span non-uniform bridges under moving vehicles and trains by using modified beam vibration functions.
23. D. Y. ZHENG 1999 *Ph.D. Thesis. The University of Hong Kong*. Vibration and stability analysis of plate-type structures under moving loads by analytical and numerical methods.
24. Y. K. CHEUNG, F. T. K. AU and D. Y. ZHENG 2000 *Thin-Walled Structures* **36**, 89–110. Finite strip method for the free vibration and buckling analysis of plates with abrupt changes in thickness and complex support conditions.
25. J. Y. LIU, D. Y. ZHENG and Z. J. MEI 1995 *Practical Integral Transforms in Engineering* (in Chinese). Wuhan, P.R. China: Huazhong University of Science and Technology Press.
26. D. J. DAWE and S. WANG 1992 *International Journal for Numerical Methods in Engineering* **33**, 819–844. Vibration of shear-deformable beams using a spline-function approach.

27. S. WANG 1997 *International Journal for Numerical Methods in Engineering* **40**, 473–491. A unified Timoshenko beam B-spline Rayleigh–Ritz method for vibration and buckling analysis of thick and thin beams and plates.
28. M. KISA, J. BRANDON and M. TOPCU 1998 *Computers and Structures* **67**, 215–223. Free vibration analysis of cracked beams by a combination of finite elements and component mode synthesis methods.
29. D. Y. ZHENG and S. C. FAN *Journal of Sound and Vibration* **242**, 701–717. Natural frequencies of a non-uniform beam with multiple cracks via modified Fourier series.

APPENDIX A: NOMENCLATURE

E	Young's elastic modulus
μ	the Poisson ratio
ρ	density of mass
G	shear modulus
k'	cross-section coefficient
λ	axial-force coefficient
$N(y)$	axial-force function
$\bar{Y}_m(y)$	basic Fourier series
$\tilde{Y}_m(y)$	augmenting piecewise constant function
$Y_m(y)$	modified Fourier series
$Q-1$	number of transverse open cracks
$\{y_i, i=1, 2, \ldots, Q+1\}$	y-ordinates for endpoint at LHS, location of cracks and endpoint at RHS of beam
$\{s_i, i=1, 2, \ldots, N_0\}$	y-ordinates of point-spring supports
$A(y)$	cross-sectional area of beam
$I(y)$	second moment of area of cross-section
$w(y, t)$	transverse deflection of beam
$\psi(y, t)$	rotation of cross-section of beam
$\{w_m(t), \psi_m(t), m=1, \ldots, R\}$	generalized co-ordinates for deformation of beam
$\mathbf{q}_1(t)$, $\mathbf{q}_2(t)$	vectors of w_m and ψ_m respectively
r	the highest order of the basic Fourier series
R	number of terms of the modified Fourier series
ω_0	basic frequency of the basic Fourier series
$\{l_j(y), j=1, 2, \ldots, Q\}$	piecewise constant interpolation based function
$\{f_j, j=1, 2, \ldots, Q\}$	values of the augmenting piecewise constant functions
$\{a_j, j=1, 2, \ldots, Q-1\}$	depths of cracks
$\{c_j, j=1, 2, \ldots, Q-1\}$	flexibility coefficients of cracks
$\{k_i, \chi_i, i=1, \ldots, N_0\}$	translational and rotational stiffness of the point spring supports
$\mathbf{A}$	coefficient matrix for determining the augmenting function
$\mathbf{f}$	vector of the values of the augmenting piecewise constant function
$\mathbf{b}$	RHS vector for determining the augmenting function
U	total potential energy of a cracked beam
U_1	potential energy of the beam due to bending deformation
U_2	potential energy of the beam due to shearing deformation
U_3	potential energy stored in support springs
U_4	potential energy stored in the equivalent rotational springs used to model the existence of cracks
U_5	potential energy of the axial compression force
$\bar{\mathbf{H}}$	vector of the basic Fourier series function
$\tilde{\mathbf{H}}$	vector of the augmenting function
$\mathbf{H}$	vector of the modified Fourier series function
$\mathbf{K}$	total stiffness matrix for the cracked beam
$\mathbf{K}_1$	stiffness matrix corresponding to potential energy U_1
$\mathbf{K}_{21}$, $\mathbf{K}_{22}$, $\mathbf{K}_{23}$	stiffness matrix corresponding to potential energy U_2
$\mathbf{K}_{31}$, $\mathbf{K}_{32}$	stiffness matrix corresponding to potential energy U_3
$\mathbf{K}_4$	stiffness matrix corresponding to potential energy U_4
$\mathbf{K}_G$	stiffness matrix corresponding to potential energy U_5

T	total kinetic energy of the beam
T_1	kinetic energy of the beam due to transverse deflection movement
T_2	kinetic energy of the beam due to rotation movement
$\mathbf{M}$	total mass matrix of the beam
$\mathbf{M}_1$	mass matrix of the beam corresponding to T_1
$\mathbf{M}_2$	mass matrix of the beam corresponding to T_2
L	Lagrangian function